

ARTICLES

Order and Dynamics of a Liquid Crystalline Dendrimer by Means of ^2H NMR Spectroscopy

Valentina Domenici,^{*,†} Mario Cifelli,[†] Carlo Alberto Veracini,[†] Natalia I. Boiko,[‡] Elena V. Agina,[‡] and Valery P. Shibaev[‡]

Dipartimento di Chimica e Chimica Industriale, Università di Pisa, Via Risorgimento 35, 56126, Italy and Chemistry Department, Moscow State University, Moscow 119992, Russia

Received: January 13, 2008; Revised Manuscript Received: September 18, 2008

A complete Deuterium NMR study performed on partially deuterated liquid crystalline carbosilane dendrimer is here reported. The dendrimer under investigation shows a SmA phase in a large temperature range from 381 to 293 K, and its mesophasic properties have been previously determined. However, in this work the occurrence of a biphasic region between the isotropic and SmA phases has been put in evidence. The orientational order of the dendrimer, labeled on its lateral mesogenic units, is here evaluated in the whole temperature range by means of ^2H NMR, revealing a peculiar trend at low temperatures ($T < 326$ K). This aspect has been further investigated by a detailed analysis of the ^2H NMR spectral features, such as the quadrupolar splitting, the line shape, and the line-width, as a function of temperature. In the context of a detailed NMR analysis, relaxation times (T_1 and T_2) have also been measured, pointing out a slowing down of the dynamics by decreasing the temperature, which determines from one side the spectral changes observed in the NMR spectra, on the other the observation of a minimum in the T_1 .

Introduction

Recent years evidenced a rapid development in the field of macromolecular chemistry and physics devoted to the synthesis and characterization of liquid crystalline (LC) dendrimers, in particular, LC dendrimers containing terminal mesogenic groups.^{1–6} This interest is associated with the unusual chemical structure of these systems. In fact, on one hand, dendritic molecules have an average shape that approximates to spherical symmetry and the tendency to assume an isotropic distribution in space, because of entropic forces. On the other hand, rigid mesogenic groups tend to form anisotropic phases due to a large gain in the enthalpy. As a result of these contradictory tendencies, phase-separated and self-assembled structures should be developed.²

The investigations of LC dendrimers^{7–21} have shown that features of molecular structure, such as the generations number,^{13,14,19} chemical structure, and shape of the mesogenic groups (rod-like,⁸ disk-like,⁶ or bent-core²¹) as well as the topology of the attachment to the core (end-on and side-on) predetermine their ability to display the mesomorphism.^{9,11} For example, LC dendrimers can form nematic^{15,18} and lamellar smectic mesophases, as a result of the terminal mesogenic groups interaction,^{12,20,21} and different types of columnar mesophases, as a result of individual macromolecules interaction.^{13,14,19} Moreover, X-ray, small angle neutron scattering (SANS), and atomic force microscopy (AFM) investigations have allowed the establishment of the change of overall shape of the LC

dendrimer molecules in different mesophases^{6,13,20–24} and revealed a complicated nanostructural organization of such compounds.

The study of hydrodynamic and electro-optical properties of dilute solutions of LC dendrimers clearly showed the dual nature of such compounds.²⁵ According to their hydrodynamic properties, LC dendrimers are similar to solid, impermeable particles. However, the chain character of the structure of these dendrimers is manifested in changes in the viscosity as a function of temperature and a small-scale mechanism of their orientation in the presence of the electric field.

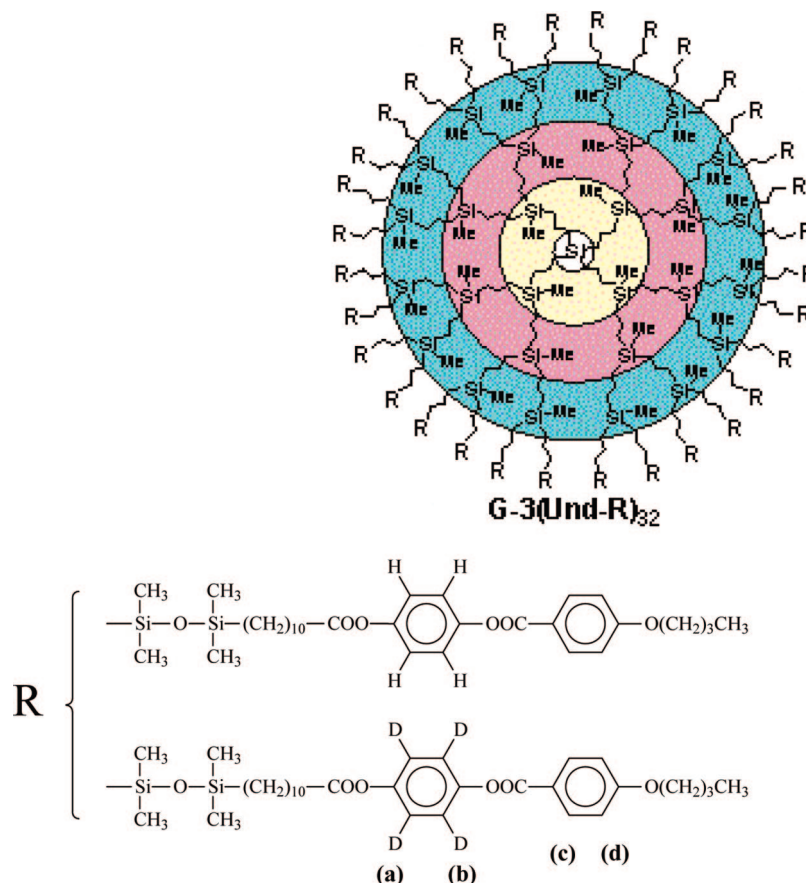
Reports on the investigations of different dendrimers have already appeared,^{19,26} and their supramolecular liquid crystalline organization has also been studied. In this context, one of the most informative techniques for studying molecular order and dynamics in LC polymers is indeed NMR spectroscopy, allowing the investigation of the orientation, structure, and dynamics processes under the effect of the external magnetic field.^{27–34} In particular, ^2H NMR has been extensively used for studying liquid crystals and liquid crystalline polymers in suitably isotopically enriched samples.^{35–38} As in this case, ^2H NMR spectra are substantially simplified as only the deuterated sites in the molecule are investigated. From the orientation of the quadrupolar tensor of the C–D bond under investigation, detailed information can be extracted on the molecular order of deuterated molecular fragments,³⁹ and relaxation studies can provide valuable information on the dynamic processes, that is, collective motions, whole molecule reorientations, as well as internal motions involving the deuterated fragment.³⁵ Although this approach has been used to investigated LC polymers^{40,41} at the present, to our best knowledge, this is the

* To whom correspondence should be addressed. Phone: +39 050 2219 266; fax: +39 050 2219 260; e-mail: valentin@ccci.unipi.it.

[†] Università di Pisa.

[‡] Moscow State University.

SCHEME 1: Molecular structure of the dendrimer G-3(Und-R)₃₂ under investigation. Aromatic proton–deuterium sites are denoted as a, b, c, and d. Deuterated sites are indicated as a and b, according to the text



first ^2H NMR study of selectively deuterium-labeled dendrimers forming LC phases, and there are few examples in the literature of NMR studies of LC dendrimers by means of ^1H NMR and NMR relaxometry^{42–44} and ^2H NMR of dissolved deuterated probes.⁴⁵

In this work we report the investigation of the LC carbosilane dendrimer of the third generation, with statistic distribution of protonated (50%) and deuterated (50%) terminal butoxyphenylbenzoate mesogenic groups (G-3(Und-R)₃₂) (with structural formula shown in Scheme 1) by means of ^2H NMR spectroscopy.

Experimental Methods

Materials. The synthesis of LC dendrimer under study (see Scheme 1) has been described in ref 23. The deuteration percentage on the phenyl rings of the terminal groups of the dendrimers has been checked by ^1H NMR (see Scheme 2), and it was found to be 50% within the experimental error.

In a previous paper,²³ the synthesis and a basic characterization of the G-3(Und-R)₃₂ dendrimer were reported, but SAXS data were erroneously interpreted, leading to the identification of a SmC phase, with a very small tilt angle ($<10^\circ$), instead of a SmA phase. A further analysis of the polarizing optical microscopy and wide angle X-ray spectroscopy (WAXS) data revealed the following phase transitions:

Cr 293 K SmA 381.3 K I

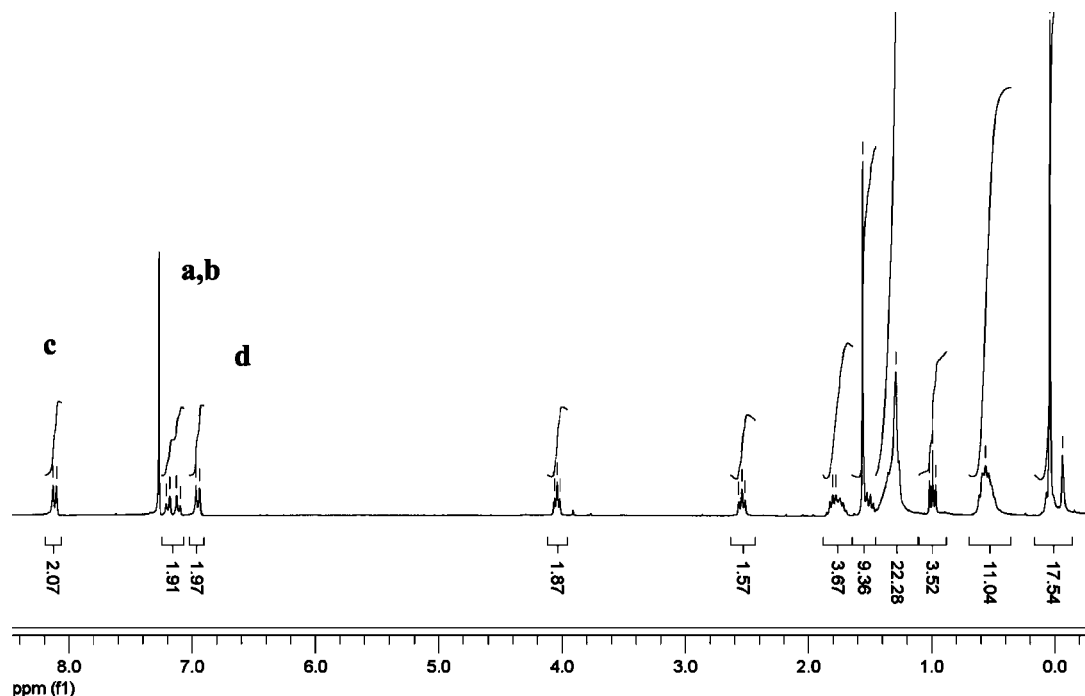
Some details of the mesomorphic characterization of the

G-3(Und-R)₃₂ dendrimer are reported in the Supporting Information.

The sample of LC dendrimer was prepared for the NMR measurements by heating it in the isotropic phase, and then it was poured in a NMR tube of 5 mm of diameter. The sample volume was about 300 mm³.

^2H NMR Measurements: The ^2H NMR experiments were carried out on a 9.40 T Varian InfinityPlus400 spectrometer, working at $\omega_0=61.3$ MHz for deuterium and a 90° pulse of 4.6 μs . The sample was macroscopically aligned within the magnet by slow cooling from the isotropic phase. The temperature was controlled within 0.2 degree. Twenty and 5 min were allowed for thermal equilibration of the sample up and below 373 K respectively, before acquiring the NMR signal. ^2H NMR static spectra were recorded either on cooling or on heating, with different rates, every one, two and five degrees from 390 to 295 K. The spectra were acquired by using the quadrupolar echo (QE) sequence ($90_x - \tau - 90_y - \tau$) with the exorcycle phase scheme,⁴⁶ without ^1H decoupling, with a τ delay of 50 μs and 120 scans. Similar measurements were also performed on a Varian XLR 300 spectrometer working at 46 MHz for deuterium with a 90° pulse of 12.5 μs .

Another experiment was carried out on the same sample cooling it from the isotropic phase outside the spectrometer in order to prevent the orientation of the sample with respect to the magnetic field.⁴⁷ Quadrupolar echo measurements were performed on the not oriented sample by heating it in the range between 297 and 347 K every 5 degrees; 50000 scans have been used.

SCHEME 2: Proton NMR spectrum of the sample G-3(Und-R)₃₂ in CDCl₃ showing that the percentage of deuteration of the sample in positions a and b ranges between 51.5 and 54%

Transverse relaxation times (T_2) were measured in the oriented phase by applying the quadrupolar echo sequence in the range between 363 K and 313 K. The variable time delay τ ranged from 20 μ s to 5 ms (22 values) and 5000 scans have been acquired for each delay. The T_2 values were determined by fitting the experimental integrals of the signal as a function of τ to the following equation that considers an exponential decay for the transverse magnetization:⁴⁶

$$I(2\tau) = I(0) \exp(-2\tau/T_2) \quad (1)$$

^2H Zeeman (T_{1Z}) and quadrupolar (T_{1Q}) longitudinal relaxation times have been measured, exploiting a broadband variance of the Jeener Broekaert experiment⁴⁸ ($90_x - \tau - 67.5_y - \tau - 45_{-x} - (\tau/2) - 45_{-x} - \alpha_0 - \tau_2 - \text{acq}$). The delay (τ) has been experimentally calibrated to produce the best antiphase quadrupolar doublet when τ_2 vanishes, and the α pulse has been set to 45° in order to maximize the quadrupolar order just before the acquisition, and spectra have been acquired accumulating from 24 to 80 scans for a good signal-to-noise ratio. A recycle delay of at least five times the maximum τ_2 value was used in order to ensure full relaxation between each scans. The variable delay τ_2 has been increased from 15 to 60 ms, and the sum (M_+) and the difference (M_-) of the integrals of the component of the quadrupolar doublet, reported as a function of the variable delay, has been used to obtain the time constants T_{1Z} and T_{1Q} , respectively, by fitting them with the two equations:

$$M_+(\tau_2) = c1 \left(1 - c2 \exp\left(-\frac{\tau_2}{T_{1Z}}\right) \right) \times$$

$$M_-(\tau_2) = c3 \exp\left(-\frac{\tau_2}{T_{1Q}}\right) + c4 \quad (2)$$

with the parameters $c1$, $c2$, $c3$, and $c4$ allowed to float in order to compensate deviations from the theoretical behavior, which

implies a complete magnetization inversion when $\tau_2 = 0$ and that $c2 = 2$ and $c4 = 0$. In all the fitting procedures, the best fitting parameters for $c2$ were in the range 2 ± 0.04 and those for $c4$ were in the range $\pm 1\%$ of the $c3$ value extrapolated at $\tau_2 = 0$. A recycle delay ranging from 0.25 to 1 s, chosen to be at least 10 times the estimated T_{1Z} value, was used in order to ensure full relaxation between each scan during the acquisitions.

Results and Discussions

The ^2H NMR spectra of the sample G-3(Und-R)₃₂, recorded by cooling it from 388 K (in the isotropic phase) to 297 K (in the crystalline phase), are reported in Figure 1. In Figure 1a the spectra from 388 to 372 K are reported for every 1 degree, with a cooling rate of about 0.1 $^\circ/\text{min}$. The temperature transition from the isotropic to the oriented phase (SmA) is found to be between 381 and 380 K. However, a biphasic region exists in a large range of temperatures, between 380 and 351 K, and it is highly reproducible. Temperature $T = 380$ K can be considered as the temperature corresponding to the formation of the first SmA domains, when the sample is cooled from the isotropic phase. Analogously, $T = 351$ K is the temperature corresponding to the total disappearance of isotropic domains, by cooling the sample. In this region, the obtained spectra are indeed characterized by a single sharp peak in the middle of the frequency range, ascribable to the isotropic phase, and a quadrupolar doublet, ascribable to the oriented phase. The large biphasic range was observed independently of the cooling/heating rate (from 0.1 to 0.04 $^\circ/\text{min}$) and we can exclude that the reasons of such phenomenon are due to instrumental problems or temperature gradients across the sample. In fact, similar measurements were performed by another spectrometer, a Varian XLR 300 working at 46 MHz for deuterium, and the biphasic region was observed with the same features (see Supporting Information). Also, the purity of the sample was checked by ^1H NMR spectroscopy (see Scheme 2) and GPC analysis (also reported in a previous paper²³) in order to exclude the presence of impurities that may cause the occurrence of

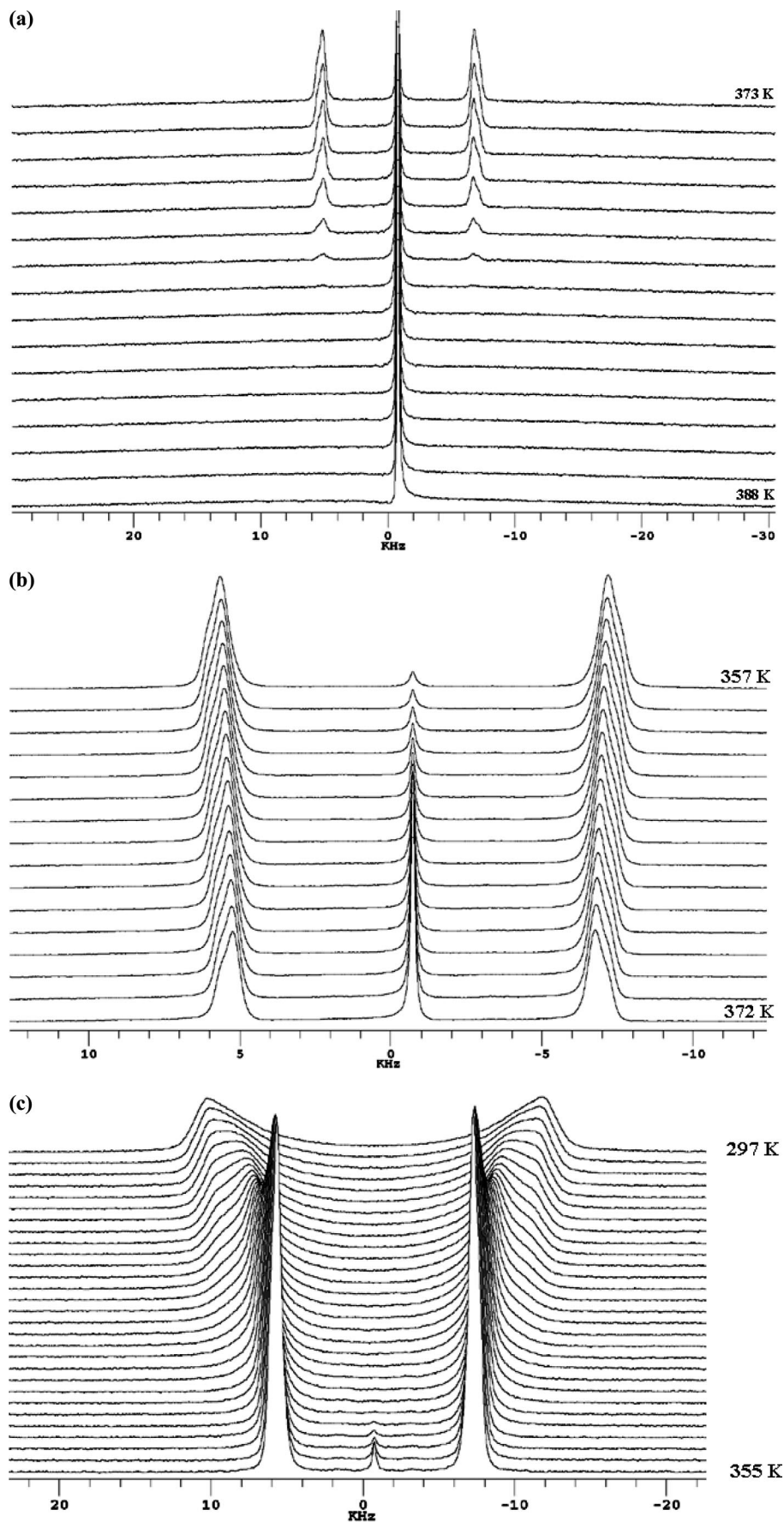
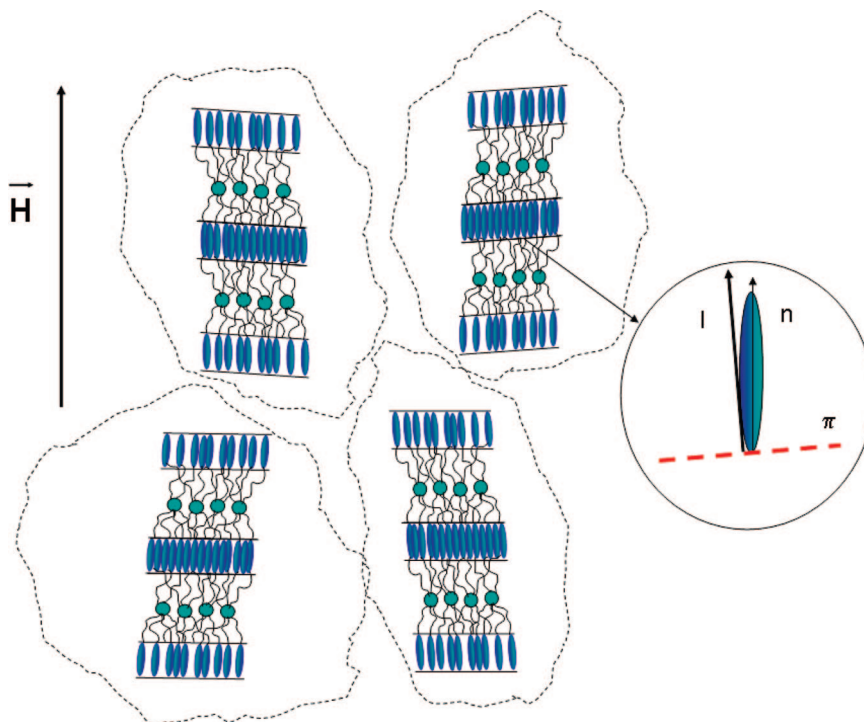


Figure 1. Series of ^2H NMR spectra of G-3(Und-R)₃₂ recorded from the isotropic to the crystalline phase. (a) Spectra from 388 to 372 K for every 1 degree. Transition from isotropic to SmA phase appears at 380 K. (b) Spectra recorded from 372 to 357 K for every 1 degree. (c) Spectra recorded from 355 to 297 K for every 2 degrees from the SmA phase to the crystalline phase.

SCHEME 3: Schematic picture of the orientation of domains with respect to the magnetic field, H . Smectic layers (π), normal to the smectic layers (l), and director (n) are shown. This scheme refers to a layered structure of the SmA phase with full overlapping among terminal LC units of dendrimers in consecutive smectic layers



biphasic regions. These observations allow us to state that the biphasic region observed by NMR is characteristic of the sample under investigation in the presence of the magnetic field and in the bulk. The reasons of such behavior may be related to the complexity of the system, which is evident from the microsegregation features typical of the structure of the SmA phase in LC dendrimers (see Scheme 3). In fact, WAXS measurements indicate that in the SmA there is an alternation between layers consisting of mesogenic groups with layers consisting of carbosilane dendritic cores. Moreover, the packing among different dendrimer macromolecules consists of a full overlapping of the terminal mesogenic units, thus giving a layered structure. The formation of domains of SmA phase may coexist with still disordered (isotropic) domains. For practical reasons we cannot exclude a very slow kinetic in the formation of the SmA domains in the bulk, and this aspect is further supported by the data reported in the Supporting Information. However, the occurrence of a biphasic region is not unusual in such complex systems, and it has also been observed in low molecular weight liquid crystals, even though the level of chemical purity was found to be 100%.^{49,50}

In Figure 1b, in which the recorded spectra are reported in the range between 372 and 357 K, the external quadrupolar doublet is much more intense than the isotropic peak, whose intensity decreases by decreasing the temperature. Figure 1c shows the ^2H NMR spectra recorded between 355 and 297 K. Spectra reported in Figures 1b and 1c were acquired with a cooling rate of 0.04 °/min. In the range 355–326 K, the spectra are characterized by a quadrupolar doublet with a similar shape as in that shown Figures 1a and 1b; on the contrary, below 326 K, the ^2H NMR spectrum evolves in a more complex one, in correspondence with a much large broadening. This spectral change is not related to any mesophasic transitions, since none of them had been revealed by other techniques (see ref 23 and the Supporting Information). Moreover, the occurrence of a precrystallization effect can be excluded based on the fact that

this spectral change is highly reproducible using different cooling/heating rates. In principle, this effect can be related to a change in the dynamic regime of motions affecting the molecular system under study with respect to the ^2H NMR time scale as well as to rearrangements and consecutive change in the supramolecular structure of the phase. The understanding of this phenomenon is the central point of this paper, and the measurements reported and discussed in the following support the hypothesis of a dynamic effect.

Concerning the spectral features of the spectra reported in Figure 1, we can observe that each peak of the quadrupolar doublet is not symmetric, as clearly shown in Figure 1b. In fact, the line shape of the signal derives from the contribution of two quadrupolar splittings, ascribable to the two deuterium couples, **a** and **b** (see Scheme 1) further split by the ^2H – ^2H dipolar coupling.⁵¹ The resulting spectral shape can be easily simulated using a suitable program.⁵² The quadrupolar splittings for the two non equivalent deuterons can be evaluated at each temperature, and they are reported in Figure 2. This simulation procedure cannot be applied below $T = 326$ K, since the spectrum is much more complicated and a large broadening occurs (see Figure 1c). At $T < 326$ K we simply report the value of the quadrupolar splittings corresponding to the two main singularities (Figure 2), which are related to different orientations of the C–D bond with respect to the magnetic field. However, these values also give an indication of the degree of the local orientational ordering when approaching the crystalline phase. It should be noticed that the trend of the quadrupolar splittings does not reach any saturation values, as well as the trend of the order parameter determined from these data in the following paragraph. This feature is quite common in LC polymers, as previously reported in several papers,^{30,47,53} and clearly distinguishes the case of macromolecular LC systems, such as dendrimers, networks, and polymers, from low molecular weight LCs.

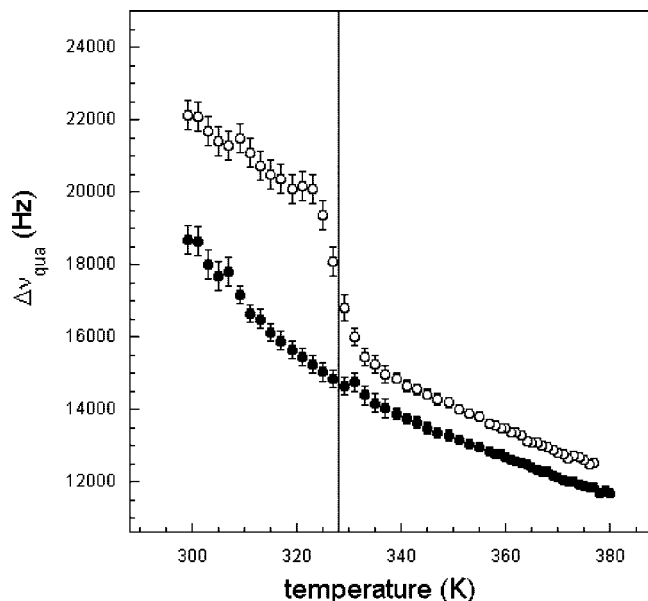


Figure 2. Experimental quadrupolar splittings of the ^2H NMR spectra of G-3(Und-R) $_{32}$ as a function of temperature. Up to $T = 326$ K, full and empty squares refer to deuterons **a** and **b**, respectively. Below this temperature, full and empty squares refer to two singularities of the recorded spectra. The experimental error is also showed.

The increasing of the value of the quadrupolar splittings, as well as of the order parameter calculated from NMR and referred to the deuterated phenyl ring, is due to the increasing of the orientational order of the SmA phase by decreasing the temperature.³⁸

From the trend of the quadrupolar splittings shown in Figure 2, it is possible to calculate the local order parameters S_{zz} and Δ_{biax} ($= S_{xx} - S_{yy}$) of the deuterated phenyl fragment (with xz being the phenyl plane and z along the *para* axis). The analysis of the experimental values has been divided into two parts.

At $T > 326$ K the two quadrupolar splittings ascribable to deuterons **a** and **b** were analyzed in a single global fitting by using the following equation:³⁶

$$\Delta\nu_q(T) = \frac{3}{2}q_{aa}\left\{S_{zz}(T)\left(\cos^2\varphi - \frac{1}{2}\sin^2\varphi - \frac{\eta}{6}\cos^2\varphi + \frac{\eta}{6} + \frac{\eta}{3}\sin^2\varphi\right) + \Delta_{\text{biax}}(T)\left(\frac{1}{2}\sin^2\varphi + \frac{\eta}{6}\cos^2\varphi + \frac{\eta}{6}\right)\right\} \quad (3)$$

where q_{aa} and η are the quadrupolar coupling constant and asymmetry parameter, respectively, and the values of $q_{aa} = 185$ kHz and $\eta = 0.04$ have been fixed as constants from the literature.³⁶ This analysis is based on the commonly accepted assumptions^{30,47,53} that the symmetry of the phenyl fragment is cylindrical, with the cylindrical axis coincident with the *para* axis, and that the oriented SmA phase is a uniaxial phase. For *para*-disubstituted aromatic rings the principal reference frame of the order tensor has its x and z axes in the ring plane, with z along the *para* direction. In this analysis, Δ_{biax} is considered temperature independent,^{36,38} and its constant value is obtained directly from the fitting. The angle (φ) between the C–D bonds and the z direction, one for each deuterium, has also been determined from the fitting, allowing small geometrical distortions of the phenyl moiety. The best-fitting values of the global analysis of the two quadrupolar splittings at $T > 326$ K gives rise to $\Delta_{\text{biax}} = 0.001$ (a very small fragment biaxiality), $\varphi_a = 59.4^\circ$, and $\varphi_b = 59.7^\circ$ (small geometrical distortions) and to

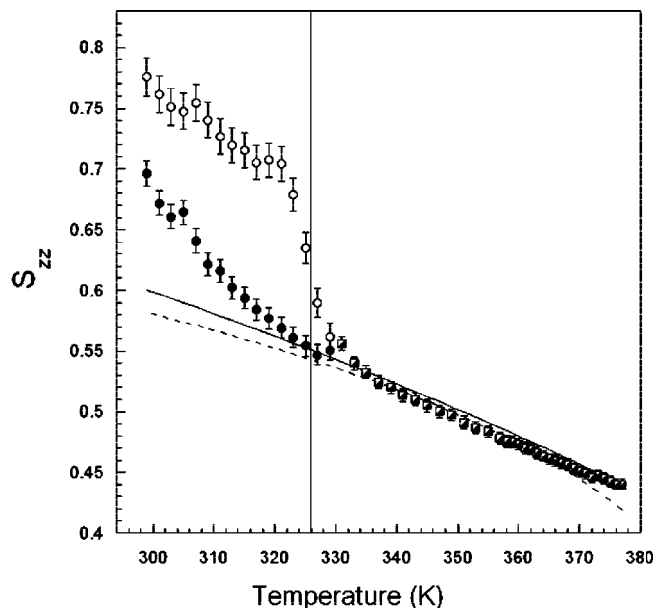


Figure 3. Orientational order parameter S_{zz} referred to the deuterated phenyl moiety of G-3(Und-R) $_{32}$ calculated according to eq 3. Squares are obtained from the quadrupolar splittings of the **a** and **b** deuterons in a global fitting. Full and empty circles refer to the order parameters obtained from the two spectral singularities below $T = 326$ K. Dashed and solid curves are the best-fitted values of the order parameter at high temperature according to eqs 4 and 5.

the values of the order parameter $S_{zz}(T)$ reported in Figure 3 (squares). We have observed that the fitting is not altered in the best-fitting values if we fix the phenyl biaxiality equal to zero. This result confirms that the phenyl fragment is uniaxial in our system at $T > 326$ K. The range of local orientational order S_{zz} is 0.44–0.56 at higher temperatures. These values of S_{zz} are lower with respect to data available for typical smectic A phases,³⁸ but we should point out that the whole trend of S_{zz} is different with respect to that of rod-like liquid crystals. This fact, and the occurrence of a large biphasic region, may explain why these data cannot be completely described by the standard theories, such as the McMillan one.⁵⁴

At $T < 326$ K, from the quadrupolar splittings corresponding to the two singularities of the spectra shown in Figure 1c, the local order parameter S_{zz} was calculated using eq 3, assuming that the fragment biaxiality is null (similarly to higher temperatures). These values, also reported in Figure 3, have a different meaning with respect to the values of S_{zz} obtained at higher temperatures, since they simply give the range of the local order parameter, ΔS_{zz} , related to the different orientation of the C–D bonds with respect to the magnetic field. Moreover, at this stage, a partial misalignment of the local directors cannot be excluded. The values of S_{zz} ranging between 0.70 and 0.78 at room temperature indicate a quite high degree of orientational order, typical of SmA phases.³⁸

As for the trend of the quadrupolar splittings, the values of S_{zz} do not tend to any saturation value. In fact, even though we limit our analysis to the range of stability of the SmA phase from 381 to 326 K, the simple Haller equation⁵⁵ is not able to describe the trend of S_{zz} (see dashed curve in Figure 3).

$$S(T) = S_0(1 - T/T^*)^\gamma \quad (4)$$

A better fitting is obtained by using the modified Landau-de Gennes equation,⁵⁶ shown below:

$$S(T) = S_0((1 - T/T^*)/(1 - \tilde{T}/T^*))^\gamma \quad (5)$$

The solid curve shown in Figure 5 refers to the best fitting of the experimental data using eq 5, which basically consists in having introduced a second transition to a glasslike phase, occurring at $T = \tilde{T}$, which was found to be 298.5 K, according to the best-fitting parameters, and it corresponds to the SmA–crystalline mesophase transition within the experimental error. This second transition is in addition to the first transition, at $T = T^*$, in both Haller and modified-Haller equations, which refers to the isotropic–SmA phase transition. Even though the modified Haller equation better describes the first part of the trend of S_{zz} (at higher temperatures), neither eq 4 nor eq 5 are able to describe the trend of order parameter in the whole mesophasic range until the crystalline phase is reached. This is probably due to the lack of any saturation trend, and this is a further proof that at present there are no phenomenological theories able to describe the trend of the order parameter in LC polymers.

To better understand the reasons of the spectral changes at $T < 326$ K, we investigated the spectral line broadening as well as the trend of the relaxation times.

From the analysis of ^2H NMR spectra, the trend of the line-width versus temperature can be obtained. In our case we have defined the experimental line-width as the width of the ^2H NMR signals measured at half-height, namely $\Delta\nu_{h/2}^{\text{exp}}$. The measured values of the line-width, reported in Figure 4 as a function of temperature, slightly increase by decreasing the temperature until $T = 326$ K; here, a sudden increasing occurs, thereby confirming that a change is happening in our macromolecular system. The information that can be extracted from the line-broadening is mainly related to the relaxation processes affecting the spin system under investigation. In particular, the experimental line-width $\Delta\nu_{h/2}^{\text{exp}}$ can be put in relation with the transverse relaxation time T_2 by the following relationship:

$$T_2^* = (\pi\Delta\nu_{h/2}^{\text{exp}})^{-1} \quad (6)$$

The origin of the line-broadening, and thus of the line-width, can be dynamic and/or static, and it can be expressed by eq 7

$$\Delta\nu_{h/2}^{\text{exp}} = \Delta\nu^{\text{homo}} + \Delta\nu^{\text{inhomo}} \quad (7)$$

In the case the only contribution to the line-broadening is dynamic, $\Delta\nu_{h/2}^{\text{exp}}$ is homogeneous and it can be related to the sole dynamic effects, ascribable to molecular and/or collective motions. On the contrary, if the origin of the line-width is also static, the *inhomogeneous* component of the line-broadening ($\Delta\nu^{\text{inhomo}}$) may depend on heterogeneities present in the sample and/or in the magnetic field.

To have a more quantitative description of the origin of the line-broadening, we have measured the transverse relaxation time T_2 using the QE pulse sequence.⁴⁶ The obtained T_2 is indeed related only to the homogeneous part of the ^2H NMR line-width via $\Delta\nu^{\text{homo}} = (\pi T_2)^{-1}$.

Equation 7 can hence be rewritten as:

$$\Delta\nu_{h/2}^{\text{exp}} = \Delta\nu^{\text{homo}} + \Delta\nu^{\text{inhomo}} = \left(\frac{1}{\pi T_2} + \Delta\nu^{\text{inhomo}}\right) \quad (8)$$

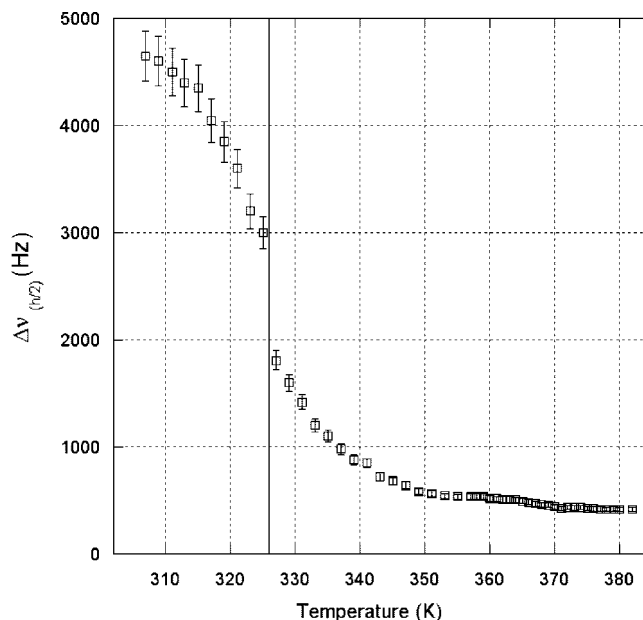


Figure 4. Experimental ^2H NMR line-width at half-height (Hz) of G-3(Und-R)₃₂ vs temperature (K). Experimental error is also reported.

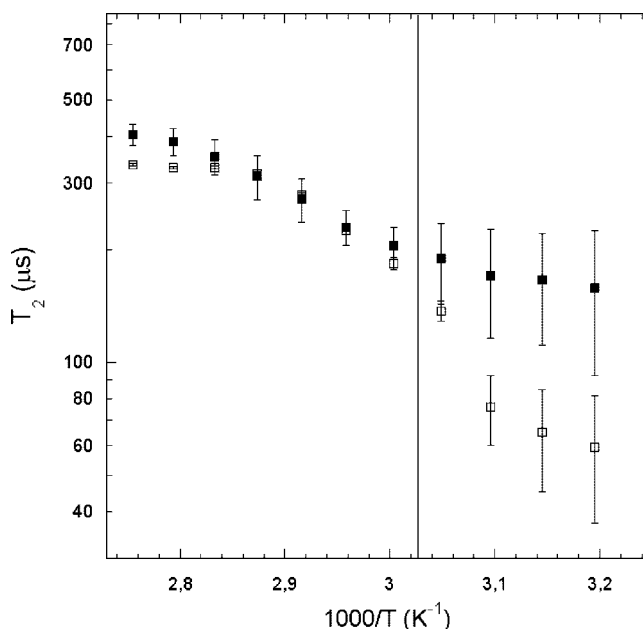


Figure 5. Spin–spin relaxation times T_2 (μs) (full squares) of G-3(Und-R)₃₂ measured by applying the QE sequence in the range from 363 to 313 K for every 5 degrees. The values of T_2^* (μs) calculated according to eq 6 from the experimental line-width $\Delta\nu_{h/2}^{\text{exp}}$ are reported in empty squares. The experimental error is also reported.

Figure 5 shows the values of T_2 , as obtained by applying eq 1 to the measured quadrupolar echo intensities decay as τ increases. Also, the values of T_2^* , calculated from the experimental line-width (the same as Figure 4) using eq 6, are reported for comparison. For simplicity the plot is in a logarithmic scale as a function of $1000/T$. In this frame, it is easy to recognize that the trend of both T_2 and T_2^* is far from being a simple line. Both trends have a “s” shape, similarly to that of the quadrupolar and line-broadening trends, centered around $T = 326$ K. This shape is more evident for the trend of T_2^* than for the T_2 , which is less pronounced. Moreover, two regions can be noticed:

(1) At $T > 326$ K (on the left of the black line in Figure 5) the values of $T_2 \approx T_2^*$, within the experimental error, thus

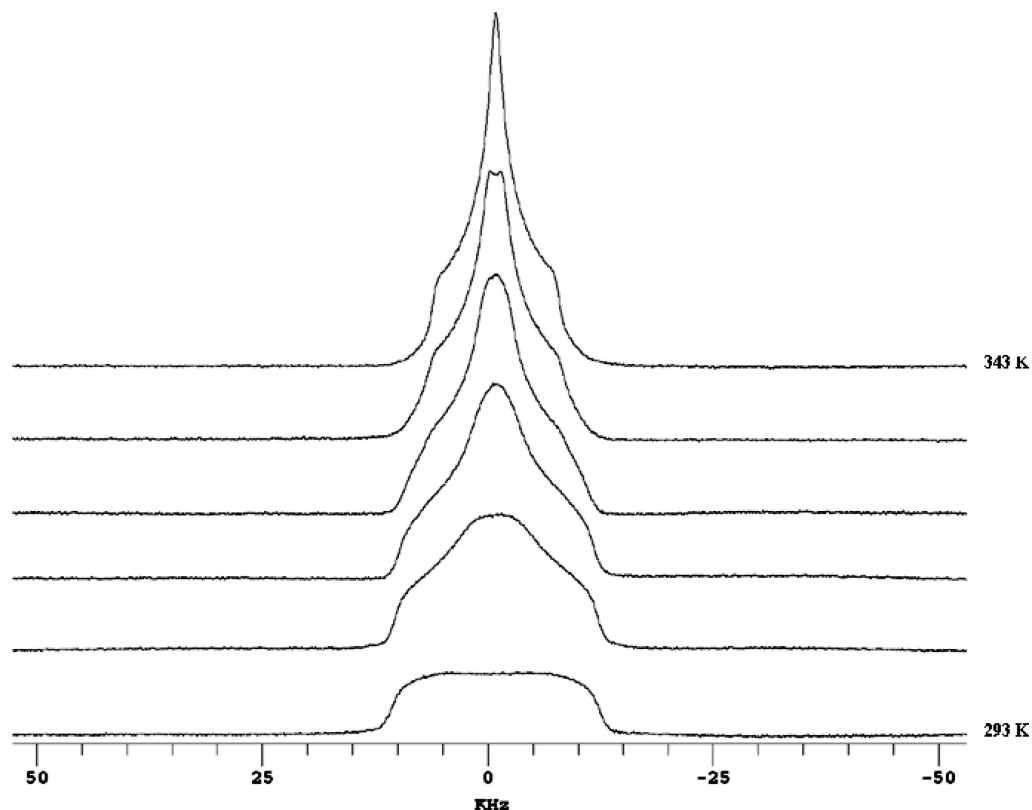


Figure 6. Series of ^2H NMR powder spectra recorded from 293 to 343 K for every 10 degrees, by heating the sample from the crystalline to the SmA phase.

indicating that the line-broadening is mainly due to dynamic processes. The inhomogeneous contribution is indeed negligible.

(2) At $T < 326\text{ K}$ (on the right of the black line in Figure 5) the experimental error associated with the evaluation of the T_2 from the QE intensities and the T_2^* from the line-width is larger than at higher temperatures. However, we can certainly state that the inhomogeneous contribution is here quite significant (in fact, $T_2 > T_2^*$). The inhomogeneous contribution to the broadening can be related to a partial disorder in the orientation of the local domains, which is indeed expected in a macromolecular system (see also the ΔS_{zz} obtained from the analysis of the quadrupolar splittings reported in Figure 3). This partial disorder is probably present to a certain extent throughout the whole smectic phase, but it appears more evident in the spectra decreasing the temperature as the molecular dynamics governing the modulation of the quadrupolar interaction slow down. If the static spectral width is defined as $\Delta\omega$, we can imagine that the correlation times of the dynamics involved start at high temperature in a regime where complete motional averaging is present, that is:

$$\Delta\omega\tau_c \ll 1 \quad (9)$$

However, as the temperature decreases we can expect that both $\Delta\omega$ and τ_c increase, and the condition expressed in eq 9 becomes less stringent, leading to an only partially averaged spectrum. This explanation is supported by the occurrence of a ΔS_{zz} as obtained from the analysis of the quadrupolar splittings and reported in Figure 3.

An additional experiment was performed on the nonoriented (powder) G-3(Und-R)₃₂ compound. The sample was heated up to the isotropic phase outside of the magnet, and then it was inserted in the magnet at room temperature. The powder

spectrum was acquired by means of the quadrupolar echo sequence⁴⁶ by heating the sample from the crystalline to the SmA phase. In these experimental conditions the magnetic field is not strong enough to uniformly orient the phase director of the SmA phase, and a powder-like spectrum due to the direct distribution is obtained. The ^2H NMR spectra acquired every 10° starting from 293 to 343 K, with an equilibration time of about 2 h, are reported in Figure 6. The narrowing of the line shape suggests the presence of a motion activated by heating the sample in the region of the investigated temperatures. This dynamic process is clearly in the intermediate regime ($\Delta\omega\tau_c \approx 1$) also at room temperature, and its effect is a partial averaging of the static powder spectrum. This process becomes faster and faster by approaching $T = 343\text{ K}$. From the trend of the quadrupolar splittings corresponding to the spectral singularities and by comparing this case to other ones reported in the literature,^{37,57,58} the value of the kinetic constant of the motion involved can be estimated to range from 10^4 to 10^7 s^{-1} by increasing the temperature. As reported for other macromolecular systems by W. H. Spiess,⁵⁸ the powder-like spectra in the intermediate regime of motions are distorted (i.e., the evaluation of the spectral singularities is indeed not straightforward), and the simulation of the line shape is much more complicated. However, the recorded spectra are quite smooth, and the lack of any sharp singularities confirm that the system is not completely homogeneous, as indicated by the comparison between the relaxation times T_2 and T_2^* . The quantitative analysis of these spectra will be the object of further investigations. At this stage we cannot exclude that the motion responsible of the spectral modulation reported in Figure 6 could be the molecular translational diffusion as well as collective motions typical of the smectic phases.

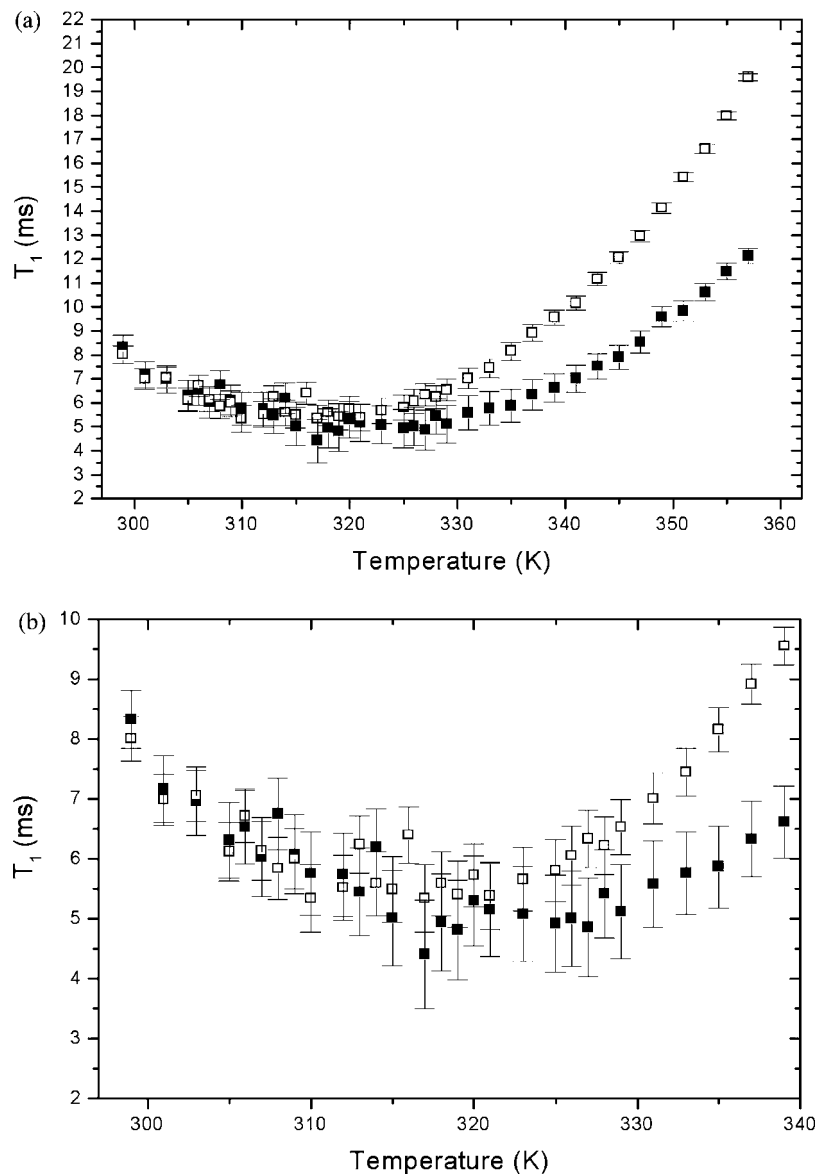


Figure 7. Spin–lattice relaxation times (ms) vs temperature (K) of G-3(Und-R)₃₂. Empty and full squares refer to T_{1Q} and T_{1Z} , respectively. Figure 7b is an enlargement of Figure 7a in order to better visualize the minimum.

In the context of a detailed investigation of the molecular dynamics of the smectic A phase also quadrupolar (T_{1Q}) and Zeeman (T_{1Z}) relaxation times have been measured according to the experimental procedure described in the Experimental Methods, and they are reported in Figure 7.

From this picture we can notice that both longitudinal relaxation times reach a minimum around $T = 326$ K, and again the dynamics involved can be framed in two different regions. For $T > 326$ K, the trend of both T_{1Q} and T_{1Z} is typical of liquid crystals in the SmA phase.³⁸ In particular, the decreasing of their values by decreasing the temperature reveals that the regime of motions responsible of the spin–lattice relaxation is fast, namely narrowing regime ($\tau_c\omega_0 < 1$). This means that the correlation time (τ_c) associated to this motion is short with respect to the inverse of the spectral frequency of the measurements. For $T < 326$ K the longitudinal relaxation times increase by decreasing the temperature, thus being in the so-called slow regime of motion for longitudinal relaxation ($\tau_c\omega_0 > 1$). This feature is not common in low molecular weight smectogens, for which the fast regime holds throughout the whole mesophasic range. A qualitative explanation is that the dynamics

responsible of the longitudinal relaxation times is slower in high molecular weight systems^{59,60} than in low molecular weight ones.

Even though the complete quantitative analysis of longitudinal relaxation times is not reported here, preliminary analyses⁵⁹ based on the small-step reorientational diffusion theory,⁶¹ and the comparison with other cases reported in the literature,^{60,62} confirmed that the main contribution to the dynamics is the internal reorientational diffusion motion of the labeled phenyl fragment. In particular, the spectral densities reported in Figure 8 as solid curves represent the best fitting of the spectra densities $J_1(\omega_0)$ and $J_2(2\omega_0)$ (symbols) calculated directly from the experimental spin–lattice relaxation times.^{38,61} The trend of the spectral densities of the dendrimer under investigation in the whole mesophasic range can be fitted only by introducing a distribution of activation energies^{60,62} for the phenyl ring reorientational motion (see Figure 8) centered in $E_a = 35$ kJ/mol with a range of distribution $\Delta E_a = \pm 10$ kJ/mol. This feature may be explained by the fact that each phenyl ring experiences a slightly different environment due to the complexity of the supramolecular structure of the dendrimer in its SmA phase and

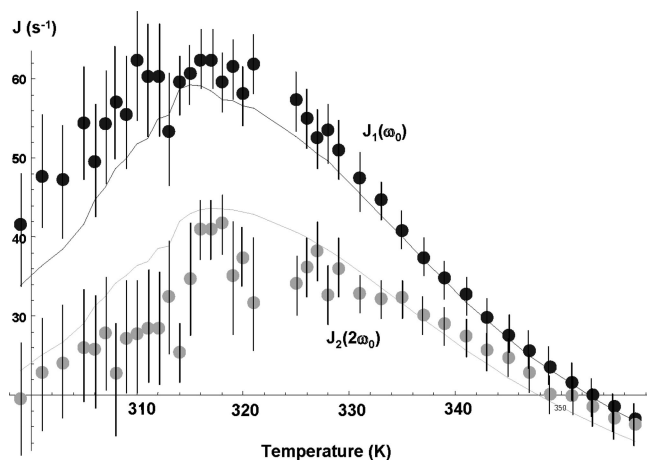


Figure 8. Spectral densities $J_1(\omega_0)$ and $J_2(2\omega_0)$ (s^{-1}) vs temperature (K). Symbols refer to the experimental spectral densities calculated from the values of T_{1Q} and T_{1Z} reported in Figure 7. Error bars are shown. Solid curves represent the spectral densities obtained by fitting the experimental ones with the small-step reorientational diffusion motion⁶¹ describing the internal motion affecting the phenyl ring.

to a partial rearrangement of the lateral mesogenic units within the smectic layers when decreasing the temperature. Now, estimating the order of magnitude of the correlation times involved in longitudinal relaxation from the relation $\tau_c \omega_0 \approx 1$ (at $T \approx 326$ K), with ω_0 being the Larmor frequency of ^2H (61.3 MHz), it turns out that $\tau_c \approx 10$ ns, which is consistent with a dynamic process that, even though being slower than in low molecular weight smectogens, still fulfills eq 9 ($\Delta\omega\tau_c \ll 1$). This observation, together with the evidence of a spread in the activation energy, confirms that the partial disorder evidenced by the analysis of spectral shapes and transverse relaxation times also affects the rotation of the deuterated phenyl rings, used to model the longitudinal relaxation.

At this stage, it is still difficult to univocally identify a specific dynamic process to be related to transverse relaxation and the broadening of spectral lines below 326 K. A reasonable hypothesis is that dynamic processes with average rates ($1/\tau_c$) of the order of the ^2H quadrupolar interaction (10–100 KHz) may be slow reorientations of the whole dendrimer, as well as collective motions, such as undulations of the smectic layers,⁴⁴ or molecular translational diffusion.

Conclusions

In this work a liquid crystal carbosilane dendrimer of the third generation, selectively deuterated on the phenyl ring of the lateral mesogenic unit, namely, G-3(Und-R)₃₂, has been investigated by ^2H NMR spectroscopy. This is the first time that several complementary ^2H NMR techniques are applied to the study of the orientational and dynamic properties of selectively labeled complex macromolecular systems such as the liquid crystalline dendrimer in question. The advantage of having a selective deuteration on the lateral phenyl ring, in particular in the ortho/meta positions, is the simplicity of the ^2H NMR spectrum and the possibility to extract, in a self-consistent way, information about the orientational ordering and dynamic properties.

The mesophasic behavior, previously investigated by other techniques, has been further studied, and it consists of a large SmA phase between the isotropic ($T = 380$ K) and the crystalline phases ($T = 293$ K). However, a large biphasic range between the isotropic and SmA phase has been observed.

The detailed NMR investigation here reported pointed out a SmA phase that, even though aligned in the magnetic field, upon cooling it from the isotropic phase still preserves an intrinsic degree of disorder due to the complexity of the macromolecular system. This heterogeneity appears from the static spectra where, together with a uniformly oriented phase, an isotropic component persists in a temperature range from the isotropic–SmA transition (380 K) to about 351 K, whereas at lower temperature a sudden broadening occurs around $T = 326$ K. The first phenomenon, in particular the existence of a large biphasic region, may also be explained by the complexity of the macromolecular system, even though a slow kinetic (not detectable by our method) cannot be ruled out. The spectral broadening can be explained by taking into account that a partial disorder in the director alignment appears and that the molecular dynamics modulating the static spectrum slow down over the limit of the complete motional narrowing ($\Delta\omega\tau_c \ll 1$).

The partial disorder of the system seems also to affect faster dynamics, as showed by the analysis of longitudinal relaxation times T_{1Z} and T_{1Q} . In this case, the spectral densities measured can be well-modeled considering a rotational dynamics of the deuterated phenyl ring with an activation energy centered at 35 KJ/mol with a range of distribution $\Delta E_a = \pm 10$ kJ/mol. Again, the spread in the activation energy can be explained considering that each phenyl ring is surrounded by a slightly different environment.

The origin of the slow dynamics affecting both the spectral line broadening and the transverse relaxation T_2 could be a molecular motion involving the whole dendrimer, such as a reorientation or the translational self-diffusion motion. Further studies are in progress in order to better clarify this point.

Acknowledgment. V.D., M.C., and C.A.V. thank the Ministry for Innovation, University and Research for the project PRIN2005 (“Modeling and characterisation of liquid crystals for nano-organised structures”), and all authors thanks the European COST projects “Functional Molecular Materials” WG D15 and “Molecular switches based on liquid crystalline materials” WG D35.

Supporting Information Available: Details of the mesomorphic behavior and experimental evidence of the appearance of the SmA phase are here reported. Additional measurements showing the thermodynamic stability of the biphasic region between the isotropic and SmA phase are shown. This information is available free of charge via the Internet at <http://pubs.acs.org>.

References and Notes

- (1) Ponomarenko, S. A.; Boiko, N. I.; Shibaev, V. P. *Polymer Science, Ser. C* **2001**, *43*, 1, and references therein.
- (2) Donnio, B.; Buathong, S.; Bury, I.; Guillon, D. *Chem. Soc. Rev.* **2007**, *36*, 1495.
- (3) Felekis, T.; Tziveleka, L.; Tsiourvas, D.; Paleos, C. M. *Macromolecules* **2005**, *38*, 1705.
- (4) Boiko, N. I.; Zhu, X.; Bobrovsky, A.; Yu., A.; Shibaev, V. P. *Chem. Mater.* **2001**, *13*, 1447.
- (5) Shibaev, V.; Bobrovsky, A.; Boiko, N. *Prog. Polym. Sci.* **2003**, *28*, 729.
- (6) Barbera, J.; Donnio, B.; Gehringer, L.; Guillon, D.; Marcos, M.; Omenat, A.; Serrano, J. L. *J. Mater. Chem.* **2005**, *15*, 4093.
- (7) Percec, V.; Chu, P.; Ungar, G.; Zhou, J. *J. Am. Chem. Soc.* **1995**, *117*, 11441.
- (8) Ponomarenko, S. A.; Rebrov, E. A.; Bobrovsky, A. Y.; Boiko, N. I.; Muzafarov, A. M.; Shibaev, V. P. *Liq. Cryst.* **1996**, *21*, 1.
- (9) Lorenz, K.; Holter, D.; Muhlaupt, R.; Frey, H. *Adv. Mater.* **1996**, *8*, 414.
- (10) Pesak, D. J.; Moore, J. S. *Angew. Chem., Int. Ed. Engl.* **1997**, *36*, 1636.

- (11) Meier, H.; Lehmann, M. *Angew. Chem., Int. Ed. Engl.* **1998**, *37*, 643.
- (12) Baars, M.W.P.L.; Sontjens, S. H.; Fischer, S. H. M.; Peerlings, H. W. I.; Meijer, E. W. *Chem.—Eur. J.* **1998**, *4*, 2456.
- (13) Ponomarenko, S. A.; Boiko, N. I.; Shibaev, V. P.; Richardson, R. M.; Whitehouse, I. J.; Rebrov, E. A.; Muzafarov, A. M. *Macromolecules* **2000**, *33*, 5549.
- (14) oiko, N.; Zhu, X.; Vinokur, R.; Rebrov, E.; Muzafarov, A.; Shibaev, V. *Ferroelectrics* **2000**, *243*, 59.
- (15) Saez, I. M.; Goodby, J. W.; Richardson, R. M. *Chem.—Eur. J.* **2001**, *7*, 2758.
- (16) Marcos, M.; Gimenez, R.; Serrano, J. L.; Donnio, B.; Heinrich, B.; Guillon, D. *Chem.—Eur. J.* **2001**, *7*, 1006.
- (17) Elsaber, R. H.; Mehl, G.; Goodby, J. W.; Veith, M. *Angew. Chem., Int. Ed. Engl.* **2001**, *40*, 2688.
- (18) Barbera, J.; Gimenez, R.; Marcos, M.; Serrano, J. L. *Liq. Cryst.* **2002**, *29*, 309.
- (19) Rueff, J. M.; Barbera, J.; Donnio, B.; Guillon, D.; Marcos, M.; Serrano, J. L. *Macromolecules* **2003**, *36*, 8368.
- (20) Boiko, N. I.; Lysachkov, A. I.; Ponomarenko, S. A.; Shibaev, V. P.; Richardson, R. M. *Colloid Polym. Sci.* **2005**, *283*, 1155.
- (21) Kosata, B.; Tamba, G.-M.; Baumeister, U.; Pelz, K.; Diele, S.; Pezl, G.; Galli, G.; Samaritani, S.; Agina, E. V.; Boiko, N. I.; Shibaev, V. P.; Weissflog, W. *Chem. Mater.* **2006**, *18*, 691.
- (22) Ponomarenko, S. A.; Boiko, N. I.; Shibaev, V. P.; Magonov, S. N. *Langmuir* **2000**, *16*, 5487.
- (23) Agina, E. V.; Boiko, N. I.; Richardson, R. M.; Ostrovskii, B. I.; Shibaev, V. P.; Rebrov, E. A.; Muzafarov, A. M. *Polymer Science, Ser. A* **2007**, *49*, 412.
- (24) Genson, K. L.; Holzmüller, J.; Leshchiner, I.; Agina, E. V.; Boiko, N.; Shibaev, V.; Tsukruk, V. *Macromol.* **2005**, *38*, 8028.
- (25) Ryumtsev, E. I.; Evlampieva, N. P.; Lezov, A. V.; Ponomarenko, S. A.; Boiko, N. I.; Shibaev, V. P. *Liq. Cryst.* **1998**, *25*, 475.
- (26) Martin-Rapun, R.; Marcos, M.; Omenat, A.; Serrano, J. L.; Luckhurst, G. R.; Mainal, A. *Chem. Mater.* **2004**, *16*, 4969.
- (27) Shibaev, V. P. *Mol. Cryst. Liq. Cryst.* **1994**, *243*, 201.
- (28) Moore, J. S.; Stupp, S. I. *Macromol.* **1987**, *20*, 282.
- (29) Esnault, P.; Casquilho, J. P.; Volino, F.; Martins, A. F.; Blumstein, A. *Liq. Cryst.* **1990**, *7*, 607.
- (30) Barmatov, E.; Chiezzì, L.; Pizzanelli, S.; Veracini, C. A. *Macromol.* **2002**, *35*, 3076.
- (31) Geib, H.; Hisgen, B.; Pschorn, U.; Ringsdorf, H.; Spiess, H. W. *J. Am. Chem. Soc.* **1982**, *104*, 917.
- (32) Boeffel, C.; Hisgen, B.; Pschorn, U.; Ringsdorf, H.; Spiess, H. W. *Isr. J. Chem.* **1983**, *23*, 388.
- (33) Boeffel, C.; Spiess, H. W. *Macromol.* **1988**, *21*, 1626.
- (34) Germano, G.; Veracini, C. A.; Boeffel, C.; Spiess, H. W. *Mol. Cryst. Liq. Cryst.* **1995**, *266*, 47.
- (35) Dong, R. Y. *Prog. Nucl. Magn. Reson. Spectrosc.* **2002**, *41*, 115.
- (36) Veracini, C. A. NMR Spectra in Liquid Crystals the Partially Averaged Spin Hamiltonian. In *Nuclear Magnetic Resonance of Liquid Crystals*; Emsley, J. W. Ed.; Reidel: Dordrecht, 1985; Vol. 141, Ch. 5.
- (37) Schmith-Rohr, K.; Spiess, H. W. In *Multidimensional Solid State NMR and Polymers*; Academic Press: London, 1994; Chapters 6–9.
- (38) Domenici, V.; Geppi, M.; Veracini, C. A. *Prog. Nucl. Magn. Reson. Spectrosc.* **2007**, *50*, 1.
- (39) Abragam, A. *Principles of Nuclear Magnetism*; Oxford University Press: New York, 1961.
- (40) Ebelhauser, R.; Fahmy, T.; Spiess, H. W. *Macromol. Rapid Commun.* **2003**, *5*, 333.
- (41) Kornfield, J. A.; Spiess, H. W.; Neftzger, H.; Eisenbach, C. D. *Macromol.* **1991**, *24*, 4787.
- (42) Van-Quynh, A. A.; Filip, D.; Cruz, C.; Sebastião, P. J.; Ribeiro, A. C.; Rueff, J.-M.; Marcos, M.; Serrano, L. J. *Mol. Cryst. Liq. Cryst.* **2006**, *450*, 191.
- (43) Filip, D.; Cruz, C.; Sebastião, P. J.; Ribeiro, A. C.; Vilfan, M.; Meyer, T.; Kouwer, P. H. J.; Mehl, G. H. *Phys. Rev. E* **2007**, *75*, 11704.
- (44) Van-Quynh, A.; Filip, D.; Cruz, C.; Sebastião, P. J.; Ribeiro, A. C.; Rueff, J.-M.; Marcos, M.; Serrano, J. L. *Eur. Phys. J. E* **2005**, *18*, 149.
- (45) Martin-Rapun, R.; Marcos, M.; Omenat, A.; Serrano, J. L.; Luckhurst, G. R.; Mainal, A. *Chem. Mater.* **2004**, *16*, 4969.
- (46) Luz, Z.; Meiboom, S. J. *Chem. Phys.* **1963**, *39*, 366.
- (47) Catalano, D.; Chiezzì, L.; Domenici, V.; Galli, G.; Veracini, C. A. *Mol. Cryst. Liq. Cryst.* **2003**, *398*, 127.
- (48) Wimperis, S. J. *Magn. Reson.* **1990**, *86*, 46.
- (49) Catalano, D.; Domenici, V.; Marini, A.; Veracini, C. A.; Bubnov, A.; Glogarova, M. *J. Phys. Chem. B* **2006**, *110*, 16459.
- (50) Domenici, V.; Veracini, C. A.; Novotna, N.; Dong, R. Y. *ChemPhysChem* **2008**, *9*, 556.
- (51) Hsi, S.; Zimmermann, H.; Luz, Z. *J. Chem. Phys.* **1978**, *69*, 4126.
- (52) Dichl, P.; Kellerhals, H. P.; Niederberger, W. *J. Magn. Reson.* **1971**, *4*, 352.
- (53) Chiezzì, L.; Fodor-Csorba, K.; Galli, G.; Gallot, B.; Pizzanelli, S.; Veracini, C. A. *Mol. Cryst. Liq. Cryst.* **2001**, *372*, 69.
- (54) McMillan, W. L. *Phys. Rev. A* **1971**, *4*, 1238.
- (55) Haller, I. *Prog. Solid State Chem.* **1975**, *10*, 103.
- (56) Cinacchi, G.; Domenici, V. *Phys. Rev. E* **2006**, *74*, 030701(R).
- (57) Macho, V.; Brombacher, L.; Spiess, H. W. *Appl. Magn. Reson.* **2001**, *405*, 20.
- (58) Spiess, W. H.; Sillescu, H. *J. Magn. Reson.* **1981**, *42*, 381.
- (59) Domenici, V., to be submitted.
- (60) Geppi, M.; Pizzanelli, S.; Veracini, C. A. *Chem. Phys. Lett.* **2001**, *343*, 513.
- (61) Vold, R. R.; Vold, R. L. *J. Chem. Phys.* **1988**, *88*, 1443.
- (62) Pizzanelli, S.; *Dynamics of Anisotropic Systems by NMR* Ph.D. Thesis, University of Pisa: Italy, 2001.

JP8003085